Coupled Systems Mechanics, *Vol. 15, No. 3 (2026) 193-210*
https://doi.org/10.12989/csm.2026.15.3.193

Elastic response of an exponentially graded beam under diverse loading scenarios

Hassaine Daouadji Tahar*[1,2], Abdelaziz Hadj Henni[1,2]

[1]*Department of Civil Engineering, University of Tiaret, Algeria*
[2]*Laboratory of Geomatics and Sustainable Development, University of Tiaret, Algeria*

(Received March 24, 2026, Revised April 19, 2026, Accepted April 27, 2026)

Abstract. This paper investigates the plane stress behavior of a cantilever beam under variable bending loads, emphasizing a novel approach to modeling material properties. Unlike traditional methods, this study uses an exponential distribution to represent material properties that vary continuously through the thickness, leading to a more accurate depiction of inhomogeneous materials. The research encompasses three distinct loading scenarios: uniform, linear, and parabolic, all integrated within a cohesive plane elasticity framework. Each loading case is defined by specific parameters tailored to its characteristics. The findings of the study underscore the method's consistency and reliability, yielding results that are both accurate and satisfactory. Furthermore, the paper includes a detailed numerical example that demonstrates the profound influence of material gradation on the elastic field, reinforcing the practical significance and the overall effectiveness of the proposed modeling technique.

Keywords: elastic properties; functionally graded materials; modeling; static analysis; structural materials

1. Introduction

The analysis of functionally graded materials (FGMs) has attracted considerable attention in recent years due to their ability to enhance structural performance by smoothly varying material properties. Among these structures, beams with continuously graded properties are widely used in advanced engineering applications such as aerospace, mechanical, and civil systems, where resistance to stress concentrations and improved durability are essential. In particular, cantilever beams represent a fundamental structural element frequently subjected to bending and transverse loads, making their accurate analysis crucial for design and optimization.

In this context, the elasticity-based modeling of beams with non-homogeneous properties provides a more precise description compared to classical homogeneous assumptions. When the material properties vary exponentially through the thickness, the resulting mechanical response becomes highly sensitive to the gradation profile. This type of distribution is especially relevant in practical manufacturing processes of FGMs, where exponential laws can closely approximate real material variations. Despite the extensive literature on graded beams, most existing studies rely on simplified beam theories, which may not fully capture the two-dimensional stress state, especially under complex loading conditions. Therefore, the use of plane elasticity formulations offers a more

*Corresponding author, Professor, E-mail: daouadjitahar@gmail.com

http://www.techno-press.org/csm/5 ISSN: 2234-2184 (Print), 2234-2192 (Online)

rigorous framework for evaluating stress and displacement fields in such structures [1-11].

Beams are crucial structural members in various engineering applications, including aerospace, automotive, and ocean engineering. They can be categorized into materials and boundary conditions and solution methods. Isotropic, composite, and functionally graded beams are examples of materials used in beams. Researchers have focused on elasticity solutions for plane beams, obtaining exact and analytical solutions via Airy stress function. Mohammadimehr [12] and others have developed solutions for plane anisotropic beams, including simple tension, pure shear, and pure bending. Hayat [13] presented a general method for obtaining stress function for orthotropic beams, and Brahim [14] derived an elasticity solution for a fixed-fixed plane isotropic beam subjected to uniform load. However, the literature on the response of functionally graded beams (FGB) to mechanical and other loadings is limited. FGBs are composite materials with smooth and continuous mechanical properties, and FG beams are assumed to be isotropic materials, resulting in the same boundary conditions. Several researchers have studied the case of beam type; among them we cite as an example [15-40] team studied the response of FGPM beams, assuming material parameters to vary in a finite power series along the thickness direction. Sankar [41] and his team developed analytical methods for thermomechanical and contact analysis of FGM beams and sandwich beams with FGM cores. Zhu and Sankar [42] solved two-dimensional elasticity equations for a FGM beam subjected to transverse loads using the combined Fourier series-Galerkin method. Houari [43] presented 2D analytical solutions for plates and beams. The stress function approach is used to study a functionally graded cantilever beam under various distributed load, examining the impact of material inhomogeneity parameter on displacement and stress field [44-58].

The core contribution of the present study lies in the development of an exact analytical solution that rigorously satisfies all governing equations as well as the associated boundary conditions. This aspect represents a significant strength of the work, as exact solutions not only provide deep physical insight into structural behavior but also serve as reliable benchmark references for validating approximate and numerical methods. Consequently, this emphasis should be clearly reflected in the literature review, which ought to be structured around a critical and comprehensive synthesis of existing exact solution methodologies. In this context, prior research in the field can be systematically categorized into three major classes of universal and relatively simple exact solution approaches. The first class is the classical Fourier series solution method, which has been extensively employed in elasticity and structural analysis. This approach is based on expressing the unknown fields as trigonometric series that inherently satisfy part of the boundary conditions, thereby reducing the complexity of the problem. A notable contribution within this framework is the work of Sankar [59], who developed an elasticity solution for functionally graded beams, successfully accounting for spatial variations in material properties. The strength of this method lies in its mathematical rigor, general applicability to regularly shaped domains, and its well-established theoretical foundation. The second class comprises methods based on polynomial stress functions. In these approaches, the stress components are assumed in polynomial form, which automatically satisfies the equilibrium equations. The solution procedure then focuses on determining the unknown coefficients through the enforcement of boundary conditions. The studies by Zhong and Yu [60] fall within this category, offering efficient analytical formulations with relatively compact expressions. The main advantage of this method is its simplicity and its ability to produce closed-form solutions that are straightforward to interpret and implement. The third class involves stress function methods formulated in terms of the bending moment and its derivatives. This approach emphasizes key mechanical quantities governing flexural behavior, leading to explicit and physically transparent solutions. The work of Tang et al. [61] provides a clear illustration of this methodology, presenting an explicit determination of exact solutions for elastic rectangular beams. This method is particularly effective in capturing bending-dominated responses while maintaining analytical clarity. In summary, these three categories form the foundational framework of exact analytical solution techniques in this domain. A well-structured literature review should not only describe these approaches but also critically highlight their respective advantages, limitations, and areas of application. Such a synthesis will help to clearly position the present study within the broader research landscape and underscore its contribution to advancing exact solution methodologies.

The present study focuses on the static analysis of a cantilever beam with exponentially varying material properties subjected to different types of transverse loads. Various loading configurations, including uniform, linear, and parabolic distributions, are considered to reflect realistic service conditions. An analytical elasticity solution is developed to describe the plane stress behavior of the beam, incorporating load parameters associated with each loading case. The proposed approach aims to provide accurate insights into the influence of material gradation and loading variation on the elastic response, contributing to improved structural analysis and design of functionally graded beam systems.

2. Mathematical formulation

2.1 Mechanical properties of the E-FGM material

Functionally graded materials (FGMs) are advanced engineered materials characterized by a continuous variation of their composition and structure, achieved by gradually changing the proportions of constituent phases according to a prescribed profile. This smooth transition eliminates sharp interfaces typically found in conventional composites, thereby reducing stress concentrations and improving overall structural integrity. One of the most distinctive features of FGMs is their non-uniform microstructure, which leads to continuously varying macroscopic properties such as elasticity, thermal conductivity, and density. These characteristics make FGMs particularly attractive for applications involving severe thermal or mechanical gradients, such as in aerospace structures, thermal barrier systems, and biomedical devices.

The behavior of FGMs is commonly described through the concept of volume fraction distribution, which defines how the constituent materials are spatially arranged within the structure. Among the various mathematical models proposed in the literature, the exponential function has gained significant popularity due to its simplicity and its ability to realistically represent gradual material transitions observed in manufacturing processes. This type of gradation allows for flexible tailoring of material properties to meet specific performance requirements. In the context of structural elements, beams made of exponentially graded materials exhibit complex mechanical responses that differ significantly from those of homogeneous beams. The continuous variation of properties through the thickness influences stress distribution, deformation patterns, and overall stiffness. Therefore, understanding and accurately modeling such behavior is essential for reliable design. In this study, particular attention is devoted to cantilever beams composed of FGMs with an exponential variation of material properties. The adoption of an exponential law provides a practical and effective framework for analyzing the influence of material gradation on the elastic response of beam structures under various loading conditions.

This study examines an elastic cantilever FGM beam made of ceramic and metal, with different material properties, such as Young's modulus and Poisson's ratio, on the upper and lower surfaces.

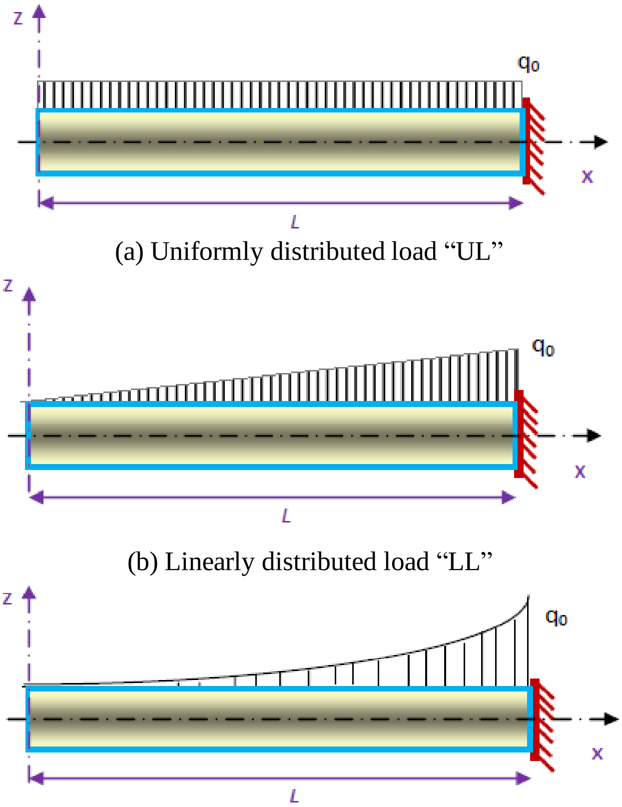

(a) Uniformly distributed load “UL”

(b) Linearly distributed load “LL”

(c) Parabolic distributed load “PL”

Figure 1. Geometries and type of loading on the cantilever FGM beam

The beams’ properties vary continuously in the thickness direction (z-axis), with Poisson’s ratio being assumed to be constant. However, the Young’s modulus in the thickness direction of the beams vary with exponential functions (E-FGM), which are generally used to describe the material properties of E-FGM.

$$E(z) = E_m . e^{k(\frac{z}{h}+\frac{1}{2})} \tag{1}$$

With:

E_m is the Young’s modulus for aluminum and k represents the coefficient of degree of homogeneity of the material

2.2 Analytical formulation of basic equations: problem description

A cantilever FGM beam of uniform thickness h is described using a Cartesian coordinate system, with upper and lower surfaces in the plane z=h/2 and -z=h/2. The beam’s edges are denoted by L and b, and it is assumed to be in a plane stress state normal to the x–z plane and subjected to three type load q(x) on its upper surface applied separately, namely a uniformly distributed load, linearly distributed load and parabolic distributed load, whose expression for the load q(x) is given by Eq. (2), with material properties varying in the thickness direction.

Where:

$$q(x) = q_0(\alpha_0 + \alpha_1 \frac{x}{l} + \alpha_2 \frac{x^2}{l^2}) \tag{2}$$

and q_0: is the load amplitude

α_i (i=0; 1; 2): load parameter. (Fig. 1)

α_0 : uniformly distributed load “UL” (Fig. 1(a))

α_1 : linearly distributed load “LL” (Fig. 1(b))

α_2 : Parabolic distributed load “PL” (Fig. 1(c))

In the absence of body forces the equilibrium equations are given as:

$$\begin{gathered}\frac{\partial \sigma_x}{\partial x} + \frac{\partial \tau_{xz}}{\partial z} = 0, \\ \frac{\partial \tau_{xz}}{\partial x} + \frac{\partial \sigma_z}{\partial z} = 0\end{gathered} \tag{3}$$

where σ_x, σ_z, τ_{xz} are stress components.

The relationships between strains and displacements are:

$$\begin{aligned}\varepsilon_x &= \frac{\partial u}{\partial x}, \\ \varepsilon_z &= \frac{\partial w}{\partial z}, \\ \gamma_{xz} &= \frac{\partial u}{\partial z} + \frac{\partial w}{\partial x}\end{aligned} \tag{4}$$

where u, w are displacement components, ε_x, ε_z, γ_{xz} are strain components that should satisfy the following strain compatibility equation:

$$\frac{\partial^2 \varepsilon_x}{\partial z^2} + \frac{\partial^2 \varepsilon_z}{\partial x^2} - \frac{\partial^2 \gamma_{xz}}{\partial x \, \partial z} = 0 \tag{5}$$

The constitutive relations of orthotropic FGM are

$$\begin{aligned}\varepsilon_x &= S_{11}\sigma_x + S_{13}\sigma_z, \\ \varepsilon_z &= S_{13}\sigma_x + S_{33}\sigma_z, \\ \gamma_{xz} &= S_{44}\tau_{xz}\end{aligned} \tag{6}$$

where S_{11}, S_{33}, S_{13}, S_{44} are the elastic compliance parameters given by:

$$\begin{aligned}S_{11} &= S_{33} = \frac{1}{E(z)}, \\ S_{13} &= -\frac{\nu}{E(z)}, \\ S_{44} &= \frac{2(1+\nu)}{E(z)}\end{aligned} \tag{7}$$

The boundary conditions of elasticity at the upper and lower surfaces are:

$$\begin{gathered}\sigma_z(x, +h/2) = -q(x), \\ \sigma_z(x, -h/2) = 0, \\ \tau_{xz}(x, \pm h/2) = 0\end{gathered} \tag{8}$$

The boundary conditions at the left end (free) of the FGM beam are:

$$N_0 = 0,$$

$$M_0 = 0,\quad Q_0 = 0 \tag{9}$$

where $N_0$and M_0 denote the axial force, moment and shear force at $x = 0$. The boundary conditions for the fixed end at the right end (fixed) of the beam are taken as:

$$u = w = 0,\quad \frac{\partial w}{\partial x} = 0 \ \text{ at } x = L,\ z = 0 \tag{10}$$

2.3 Elasticity solution

In order to obtain a general solution to Eqs. (5)-(12), Airy stress function $\xi(x,z)$ is introduced such that

$$\sigma_x = \frac{\partial^2 \xi}{\partial z^2},\quad \sigma_z = \frac{\partial^2 \xi}{\partial x^2},\quad \tau_{xz} = -\frac{\partial^2 \xi}{\partial x\, \partial z} \tag{11}$$

So that Eq. (5) is satisfied automatically. We then assume that:

$$\xi(x,z) = \xi_0(z) + x\xi_1(z) + x^2\xi_2(z) + x^3\xi_3(z) + x^4\xi_4(z) \tag{12}$$

where $\xi_0(z)$, $\xi_1(z)$ and $\xi_2(z)$ are unknown functions to be determined. Substitution of Eq. (14) into Eq. (13) gives:

$$\sigma_x = \xi_0'' + x\xi_1'' + x^2\xi_2'' + x^3\xi_3'' + x^4\xi_4'', \tag{13a}$$

$$\sigma_z = 2\xi_2 + 6x\xi_3 + 12x^2\xi_4, \tag{13b}$$

$$\tau_{xz} = -\left(\xi_1' + 2x\xi_2' + 3x^2\xi_3' + 4x^3\xi_4'\right) \tag{13c}$$

Substitution of Eq. (15) into Eq. (8), and then into Eq. (7), gives rise to

$$\left(S_{11}\xi_4''\right)'' = 0,\quad \left(S_{11}\xi_3''\right)'' = 0 \tag{14a}$$

$$\left(S_{11}\xi_1'' + 6S_{13}\xi_3\right)'' + (6S_{44}\xi_3')' + 6S_{13}\xi_3'' = 0 \tag{14b}$$

$$\left(S_{11}\xi_0'' + 2S_{13}\xi_2\right)'' + (2S_{44}\xi_2')' + 2S_{13}\xi_2'' + 24S_{33}\xi_4 = 0. \tag{14c}$$

$$\left(S_{11}\xi_2'' + 12S_{13}\xi_4\right)'' + (12S_{44}\xi_4')' + 12S_{13}\xi_4'' = 0. \tag{14d}$$

Integration of Eq. (16a) yields

$$\xi_4'' = \delta_1\Delta_1 + \delta_2\Delta_2 \tag{15a}$$

$$\xi_4' = \delta_1\Delta_1^0 + \delta_2\Delta_2^0 + \delta_3 \tag{15b}$$

$$\xi_4 = \delta_1\Delta_1^1 + \delta_2\Delta_2^1 + \delta_3 z + \delta_4 \tag{15c}$$

where and hereafter a_i ($i = 1,2,\ldots$) are integral constants, and

$$\Delta_1 = \frac{z}{S_{11}}, \tag{16a}$$

$$\Delta_2 = \frac{1}{S_{11}}, \tag{16b}$$

$$\Delta_i^n(z) = \frac{1}{n!}\int_{-h/2}^{z}(z-\eta)^n\Delta_i d\eta \quad (i = 1,2; n = 0,1) \tag{16c}$$

Integration of Eq. (16b) yields

$$\xi_3'' = \delta_5\nabla_5 + \delta_6\nabla_6 \tag{17a}$$

$$\xi_3' = \delta_5\nabla_5^0 + \delta_6\nabla_6^0 + \delta_7 \tag{17b}$$

$$\xi_3 = \delta_5\nabla_5^1 + \delta_6\nabla_6^1 + \delta_7 z + \delta_8 \tag{17c}$$

Where

$$\nabla_1 = \nabla_2 = \nabla_3 = \nabla_4 = 0, \tag{18a}$$

$$\nabla_5 = \Delta_1, \tag{18b}$$

$$\nabla_6 = \Delta_2, \tag{18c}$$

$$\nabla_i^n(z) = \frac{1}{n!}\int_{-h/2}^{z}(z-\eta)^n\nabla_i d\eta \quad (i = 5,6) \text{ and } n = 0,1 \tag{18d}$$

Substituting Eqs. (17) into Eq. (16c), and performing integration twice, we obtain

$$\xi_2'' = \sum_{i=1}^{10}\delta_i\gamma_i, \tag{19a}$$

$$\xi_2' = \sum_{i=1}^{10}\delta_i\gamma_i^0 + \delta_{11}, \tag{19b}$$

$$\xi_2 = \sum_{i=1}^{10}\delta_i\gamma_i^1 + \delta_{11}z + \delta_{12} \tag{19c}$$

Where:

$$\gamma_1 = -\frac{12S_{13}}{S_{11}}\Delta_1^1 - \frac{12}{S_{11}}\int_{-h/2}^{z}[S_{44}\Delta_1^0 + S_{13}\Delta_1(z-\eta)]d\eta, \tag{20a}$$

$$\gamma_2 = -\frac{12S_{13}}{S_{11}}\Delta_2^1 - \frac{12}{S_{11}}\int_{-h/2}^{z}[S_{44}\Delta_2^0 + S_{13}\Delta_2(z-\eta)]d\eta, \tag{20b}$$

$$\gamma_3 = -\frac{12S_{13}}{S_{11}}z - \frac{12}{S_{11}}\int_{-h/2}^{z}S_{44}d\eta, \tag{20c}$$

$$\gamma_4 = -\frac{12S_{13}}{S_{11}} \tag{20d}$$

$$\gamma_5 = \gamma_6 = \gamma_7 = \gamma_8 = 0, \tag{20e}$$

$$\gamma_9 = \Delta_1, \tag{20f}$$

$$\gamma_{10} = \Delta_2, \tag{20g}$$

$$\gamma_i^n(z) = \frac{1}{n!}\int_{-h/2}^{z}(z-\eta)^n \gamma_i d\eta \ \ (i = 1,2,\ldots,10) \text{ and } n = 0,1 \tag{21}$$

$$\xi_1^{''} = \sum_{i=1}^{14} \delta_i \chi_i, \tag{22a}$$

$$\xi_1^{'} = \sum_{i=1}^{14} \delta_i \chi_i^0 + \delta_{15}, \tag{22b}$$

$$\xi_1 = \sum_{i=1}^{14} \delta_i \chi_i^1 + \delta_{15} z + \delta_{16} \tag{22d}$$

$$\chi_5 = -\frac{6S_{13}}{S_{11}}\nabla_5^1 - \frac{6}{S_{11}}\int_{-h/2}^{z}[S_{44}\nabla_5^0 + S_{13}\nabla_5(z-\eta)]d\eta, \tag{23a}$$

$$\chi_6 = -\frac{6S_{13}}{S_{11}}\nabla_6^1 - \frac{6}{S_{11}}\int_{-h/2}^{z}[S_{44}\nabla_6^0 + S_{13}\nabla_6(z-\eta)]d\eta, \tag{23b}$$

$$\chi_7 = -\frac{6S_{13}}{S_{11}}z - \frac{6}{S_{11}}\int_{-h/2}^{z} S_{44} d\eta, \tag{23c}$$

$$\chi_8 = -\frac{6S_{13}}{S_{11}} \tag{23d}$$

$$\chi_1 = \chi_2 = \chi_3 = \chi_4 = \chi_9 = \chi_{10} = \chi_{11} = \chi_{12} = 0 \tag{23e}$$

$$\chi_{13} = \Delta_1, \tag{23f}$$

$$\chi_{14} = \delta_2, \tag{23g}$$

$$\chi_i^n(z) = \frac{1}{n!}\int_{-h/2}^{z}(z-\eta)^n \chi_i d\eta \ \ (i = 1,2,\ldots,14) \text{ and } n = 0,1 \tag{23h}$$

Substituting Eqs. (19) into Eq. (16d), and performing integration twice, we obtain

$$\xi_0^{''} = \sum_{i=1}^{17} \delta_i \lambda_i, \tag{24a}$$

where

$$\lambda_5 = \lambda_6 = \lambda_7 = \lambda_8 = 0, \tag{24b}$$

$$\lambda_1 = -\frac{12S_{13}}{S_{11}}\gamma_1^1 - \frac{2}{S_{11}}\int_{-h/2}^{z}[S_{44}\gamma_1^0 + (S_{13}\gamma_1 + 12S_{33}\Delta_1^1)(z-\eta)]d\eta, \tag{24c}$$

$$\lambda_2 = -\frac{12S_{13}}{S_{11}}\gamma_2^1 - \frac{2}{S_{11}}\int_{-h/2}^{z}[S_{44}\gamma_2^0 + (S_{13}\gamma_2 + 12S_{33}\Delta_2^1)(z-\eta)]d\eta, \tag{24d}$$

$$\lambda_3 = -\frac{2S_{13}}{S_{11}}\gamma_3^1 - \frac{2}{S_{11}}\int_{-h/2}^{z}[S_{44}\gamma_3^0 + (S_{13}\gamma_3 + 12S_{33}\eta)(z-\eta)]d\eta, \tag{24e}$$

$$\lambda_4 = -\frac{2S_{13}}{S_{11}}\gamma_4^1 - \frac{2}{S_{11}}\int_{-h/2}^{z}[S_{44}\gamma_4^0 + (S_{13}\gamma_4 + 12S_{33})(z-\eta)]d\eta, \tag{24f}$$

$$\lambda_9 = -\frac{2S_{13}}{S_{11}}\gamma_9^1 - \frac{2}{S_{11}}\int_{-h/2}^{z}[S_{44}\gamma_9^0 + S_{13}\gamma_9(z-\eta)]d\eta, \tag{24g}$$

$$\lambda_{10} = -\frac{2S_{13}}{S_{11}}\gamma_{10}^1 - \frac{2}{S_{11}}\int_{-h/2}^{z}[S_{44}\gamma_{10}^0 + S_{13}\gamma_{10}(z-\eta)]d\eta, \tag{24h}$$

$$\lambda_{11} = -\frac{2S_{13}}{S_{11}}z - \frac{2}{S_{11}}\int_{-h/2}^{z} S_{44}d\eta, \tag{24i}$$

$$\lambda_{12} = -\frac{2S_{13}}{S_{11}} \tag{24j}$$

$$\lambda_{13} = \lambda_{14} = \lambda_{15} = 0, \tag{24k}$$

$$\lambda_{16} = \Delta_1, \quad \lambda_{17} = \Delta_2, \tag{24i}$$

$$\lambda_i^n(z) = \frac{1}{n!}\int_{-h/2}^{z}(z-\eta)^n \lambda_i d\eta \ \ (i = 1,2,\ldots.,17; n = 0,1) \tag{24m}$$

The axial force N_0, bending moment M_0 and shearing force Q_0 at the left end of the beam can be obtained by integrating Eqs. (15a) and (15c) according to

$$N_0 = \int_{-h/2}^{h/2} \sigma_x(0,z)dz = \xi_0^{'}(h/2) - \xi_0^{'}(-h/2), \tag{25a}$$

$$M_0 = \int_{-h/2}^{h/2} \sigma_x(0,z)zdz = \frac{h}{2}[\xi_0^{'}(h/2) + \xi_0^{'}(-h/2)] - \xi_0(h/2) + \xi_0(-h/2), \tag{25b}$$

$$Q_0 = \int_{-h/2}^{h/2} \tau_{xz}(0,z)dz = \xi_1(-h/2) - \xi_1(h/2) \tag{25c}$$

Substitution of Eq. (15) into Eq. (10) gives

$$\xi_1^{'}(-h/2) = 0, \qquad \xi_1^{'}(h/2) = 0, \tag{26a}$$

$$\xi_2(-h/2) = 0, \qquad \xi_2^{'}(-h/2) = 0, \tag{26b}$$

$$\xi_2(h/2) = -q_0\frac{\alpha_0}{2}, \qquad \xi_2^{'}(h/2) = 0, \tag{26c}$$

$$\xi_3(-h/2) = 0, \qquad \xi_3^{'}(-h/2) = 0, \tag{26d}$$

$$\xi_3(h/2) = -q_0\frac{\alpha_1}{6L}, \qquad \xi_3^{'}(h/2) = 0, \tag{26e}$$

$$\xi_4(-h/2) = 0, \qquad \xi_4^{'}(-h/2) = 0, \tag{26f}$$

$$\xi_4(h/2) = -q_0\frac{\alpha_2}{12L^2}, \qquad \xi_4^{'}(h/2) = 0, \tag{26g}$$

Finally the integration of Eq. (8), we could obtain the displacement components as follows:

$$\begin{gathered} u = x\left(S_{11}\xi_0^{''} + 2S_{13}\xi_2\right) + \frac{x^2}{2}(S_{11}\xi_1^{''} + 6S_{13}\xi_3) + \frac{x^3}{3}(S_{11}\xi_2^{''} + 12S_{13}\xi_4) \\ + \frac{x^4}{4}S_{11}\xi_3^{''} + \frac{x^5}{5}S_{11}\xi_4^{''} - \int_{-h/2}^{z}[(z-\eta)(S_{13}\xi_1^{''} + 6S_{33}\xi_3) + S_{44}\xi_1^{'}]d\eta + \mu z + u_0, \end{gathered} \tag{27a}$$

$$\begin{gathered} w = \sum_{j=1}^{4} x^j \int_{-h/2}^{z}\left(s_{13}\xi_j^{''}\right)d\xi - \frac{\delta_5}{20}x^5 - \frac{\delta_9}{12}x^4 - \frac{\delta_{13}}{6}x^3 - \frac{\delta_{16}}{2}x^2 \\ + \int_{-h/2}^{z}[S_{33}(2\xi_2 + 6x\xi_3 + 12\xi_4)]d\eta - \mu x + w_0 \end{gathered} \tag{27b}$$

Where: u_0, w_0 and μ are integral constants.

Substituting Eqs. (17b), (17c) and (19b) into Eqs. (32e) and (32c) respectively, we have

$$\sum_{i=1}^{2} \delta_i \Delta_i^0(h/2) = 0, \tag{28a}$$

$$\sum_{i=1}^{6} \delta_i \nabla_i^0(h/2) = 0 \tag{28b}$$

$$\sum_{i=1}^{10} \delta_i \gamma_i^0(h/2) = 0 \tag{28c}$$

$$\sum_{i=1}^{14} \delta_i \chi_i^0(h/2) = 0 \tag{28d}$$

$$\sum_{i=1}^{2} \delta_i \Delta_i^1(h/2) + \frac{q_0\alpha_2}{12L^2} = 0, \tag{28e}$$

$$\sum_{i=1}^{6} \delta_i \nabla_i^1(h/2) + \frac{q_0\alpha_1}{6L} = 0 \tag{28f}$$

$$\sum_{i=1}^{10} \delta_i \gamma_i^1(h/2) + \frac{q_0\alpha_0}{2} = 0 \tag{28g}$$

$$\sum_{i=1}^{14} \delta_i \chi_i^1(h/2) = 0 \tag{28h}$$

$$\sum_{i=1}^{17} \delta_i \lambda_i^0(h/2) = 0 \tag{28i}$$

$$\sum_{i=1}^{17} \delta_i \lambda_i^1(h/2) = 0 \tag{28j}$$

Where:

$$\delta_3 = \delta_4 = \delta_7 = \delta_8 = \delta_{11} = \delta_{12} = \delta_{15} = 0 \tag{28k}$$

3. Presentations and discussion of the results

This study examines a numerical analysis of a FGM cantilever beam (L=1 m, height h=0.1 m) subjected to varying loads, with amplitude q_0=1 GPa/ml. The analysis is performed for pure materials and E-FGM materials. The Young's modulus for aluminum is 70 GPa, and Poisson's ratio is ν=0.3 on the upper surface of the beam, with the graded function assumed in E-FGM beam Eq. (1). The study parameters that we take into account in the analysis are the following:

$$\bar{w} = \frac{w}{10h} \tag{29a}$$

$$\bar{\sigma}_x = \frac{\sigma_x}{q_0} \tag{29b}$$

$$\bar{\tau}_x = \frac{\tau_x}{q_0} \tag{29c}$$

The Table 1 presents a comparative analysis of stresses and displacements for three loading types (UL, LL, PL) and varying the graduation index of FGM material, revealing the following findings.

- The uniform loading type UL showed significant stresses and displacements compared to the other two loading types, LL and PL.
- The material's degree of graduation varies, as noted in the text.
  - The most rigid material ensures stability (k=2; positive graduation) and is of significant value for the most flexible material (k=-2; negative graduation).
  - The value is highly significant for positive graduation (k=2) in normal stress.
  - The shear stress peak is recorded at the homogeneous material level, representing a plane of symmetry in FGM materials of positive and negative graduation (k=2; k=-2).

Table 1. Comparison of mid-span and free end stress results for displacements depending on the different types of loading UL, LL and PL

k	Type of Loading	$\bar{w}(0,0)$	σ_x (L/2, h/2)	τ_{xz} (L/2, 0)
-2	UL	-59,4416	37,1651	7,1252
	LL	-15,6779	6,1695	1,7828
	PL	-6,4361	1,5339	0,5953
-1	UL	-35,3036	53,2660	7,4062
	LL	-9,2910	8,8427	1,8529
	PL	-3,8027	2,1985	0,6185
0	UL	-21,225	74,7999	7,5000
	LL	-5,5785	12,3999	1,8762
	PL	-2,2791	3,0759	0,6262
1	UL	-12,9746	103,8306	7,4062
	LL	-3,4093	17,1799	1,8529
	PL	-1,3924	4,2490	0,6185
2	UL	-8,0293	143,3241	7,1252
	LL	-2,1116	23,6751	1,7828
	PL	-0,8634	5,8400	0,5953

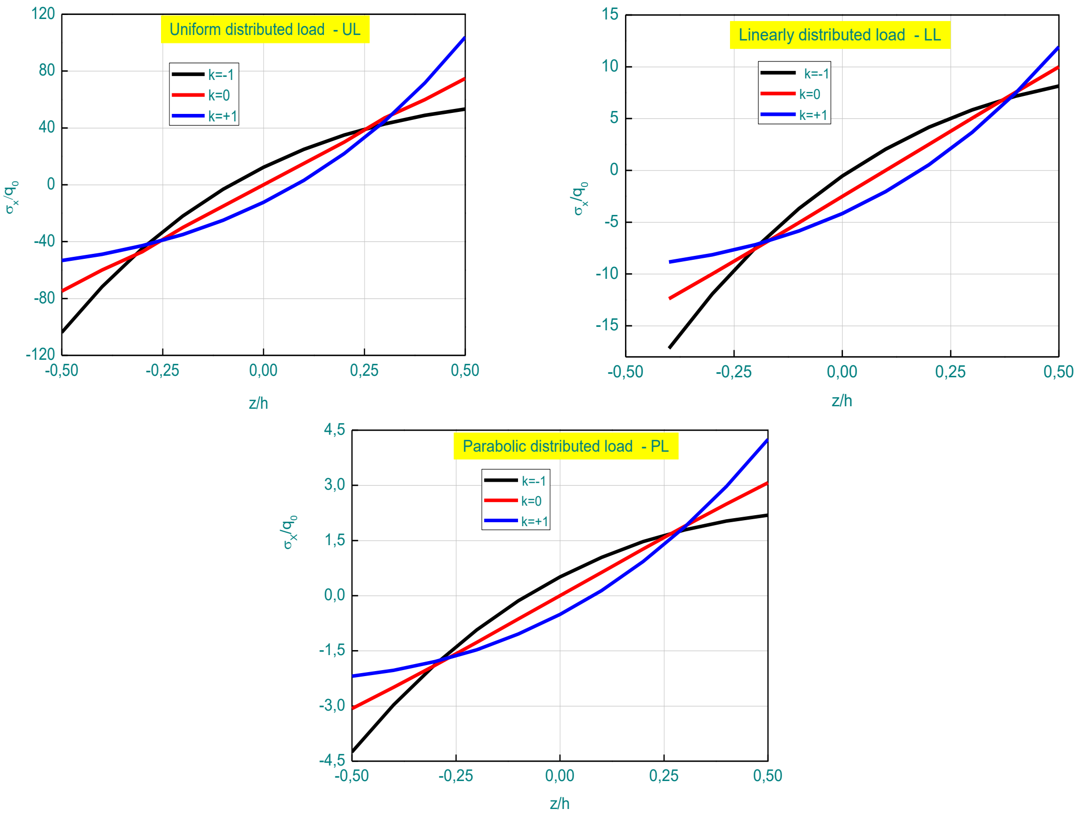

Figure 2. Dimensionless normal stress distribution across beam thickness for different loading types

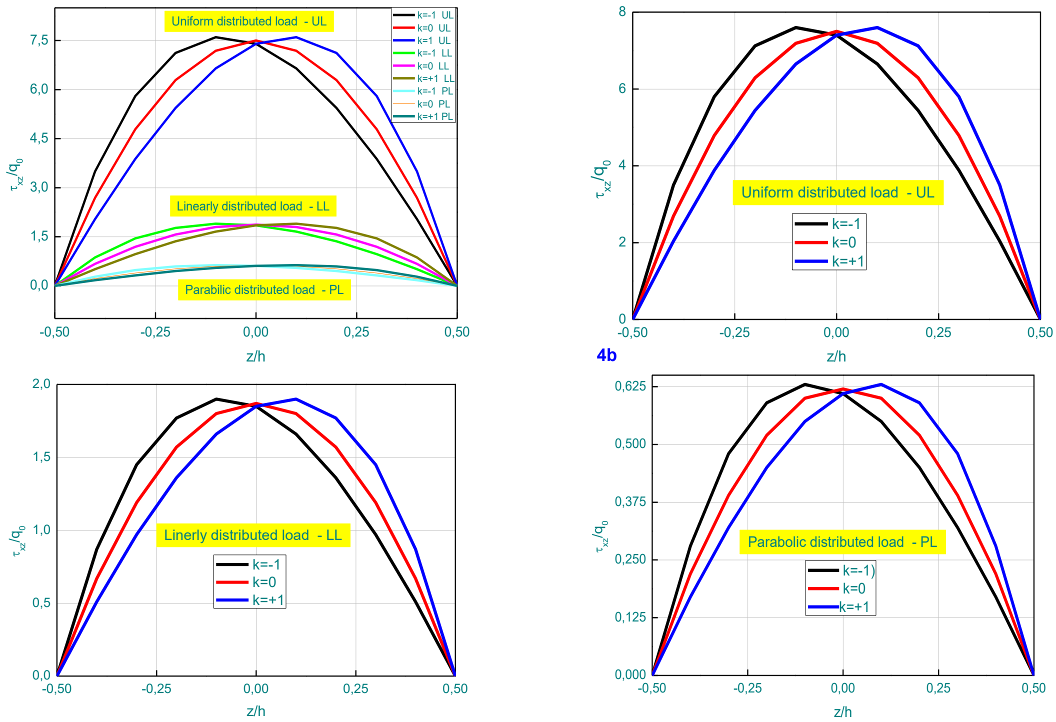

Figure 3. Dimensionless shear stress distribution across beam thickness for different loading types

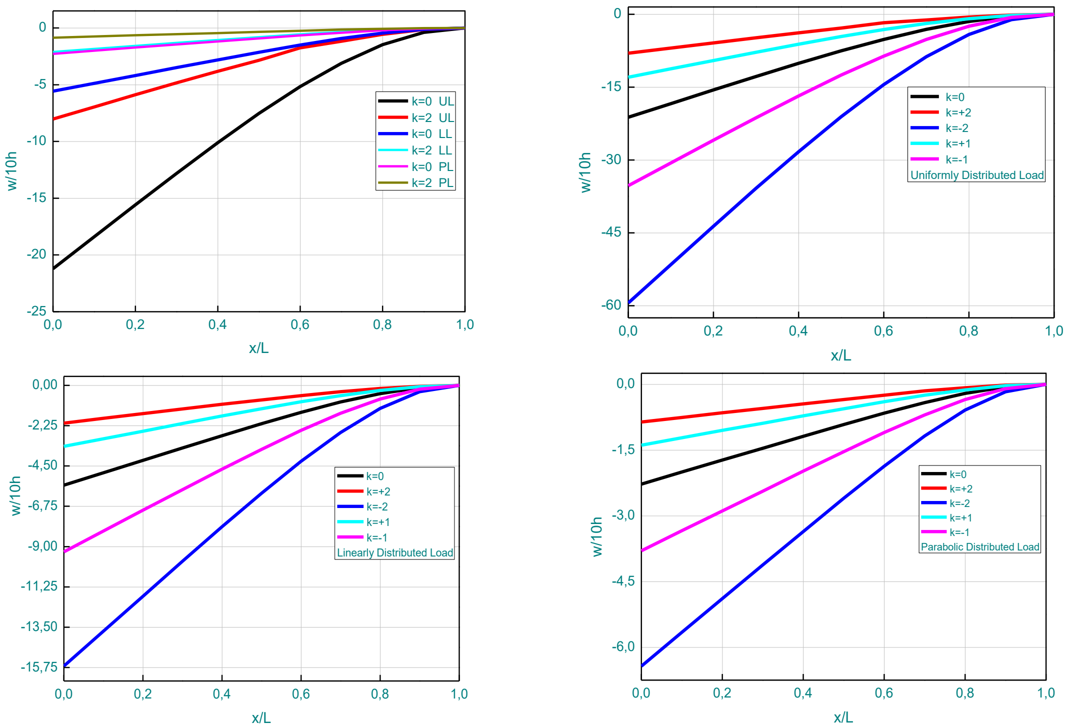

Figure 4. Variation of dimensionless displacements along the beam for different types of loading

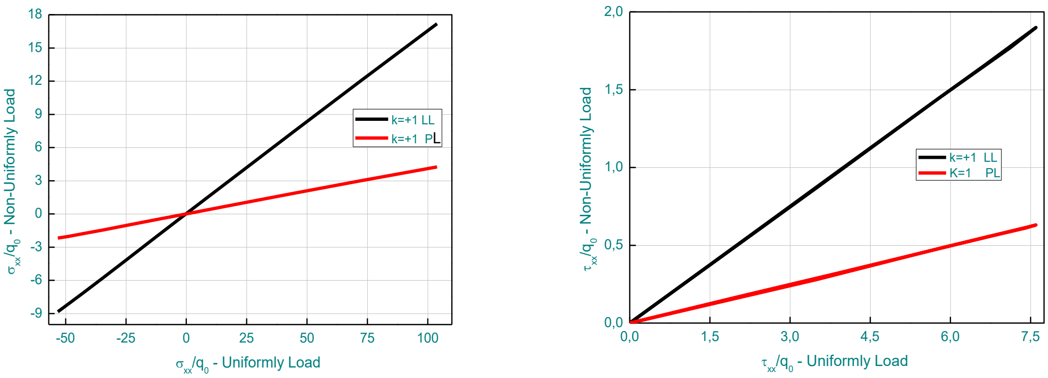

Figure 5. Relationship between non-uniform and uniform loading models for normal and shear stresses

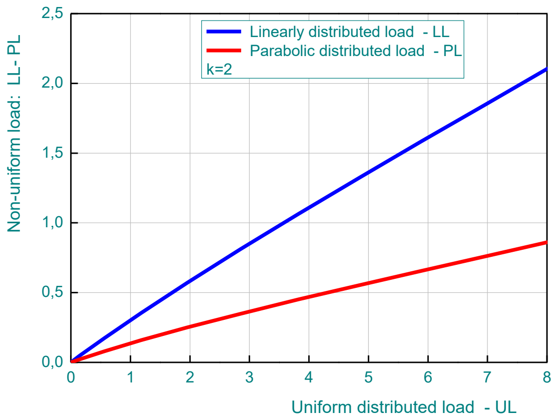

Figure 6. Relationship between the non-uniform model and the uniform loading model for the displacements of a FGM material (k=2)

Our results confirm that the more rigid the material, the greater the stability of the beam element in significant resistance.

In Fig. 2; the homogeneous model (k=0), which is linear and perfectly represents the axis of symmetry of the FGM model, is found to have the maximum value for the rigid FGM material (k=+1), which supports the conclusion drawn from the comparative study regarding the dimensionless normal stress distribution across beam thickness for different loading types.

Fig. 3 shows the dimensionless shear stress distribution across beam thickness for different loading types. The homogeneous material has a parabolically symmetrical shape, while the FGM materials have a plane of symmetry. The positive graduation of the FGM is symmetrical with respect to the negative graduation, with the peak at the level of the FGM materials compared to the homogeneous material.

Fig. 4 illustrates the variation of dimensionless displacement along the beam for various loading types, revealing the following results.

- The displacement value is crucial for uniform load UL and other loading types (LL and PL), as the rigid upper face of the FGM stabilizes the console beam.
- The importance of positive graduation, such as k=+2, in beam stability, particularly for

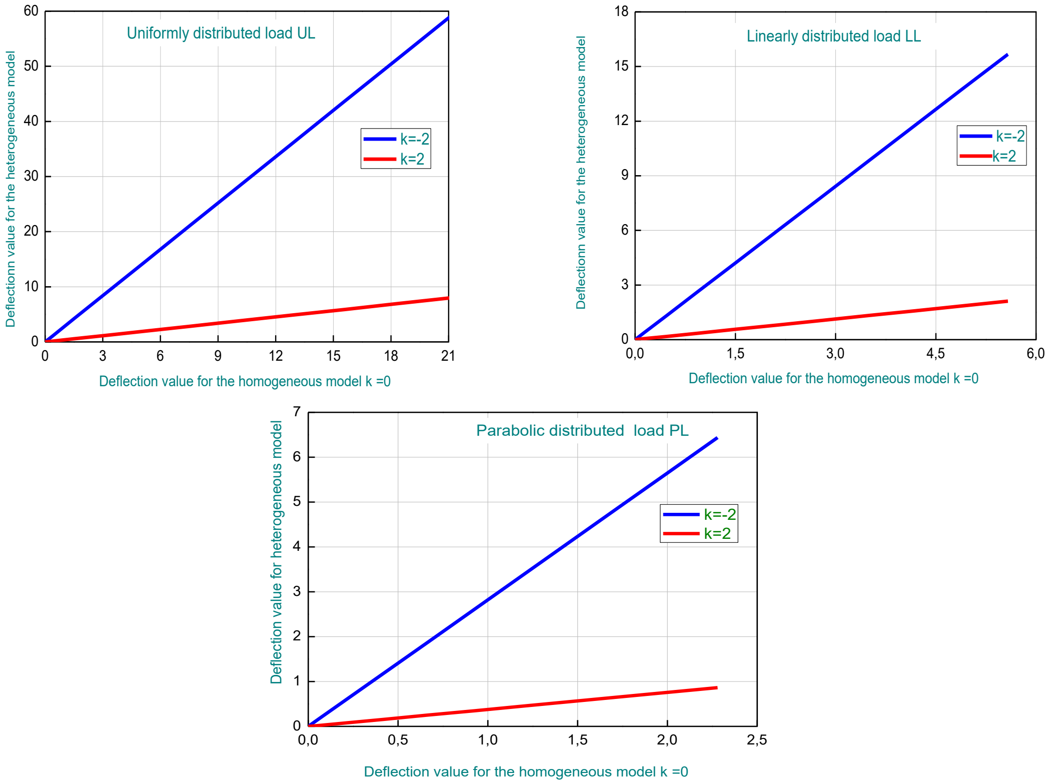

Figure 7. Relationship between the FGM model and the homogeneous model for displacements as a function of different loads

parabolic loading, is greater than negative graduation, which makes the beam instable.

The findings from the comparative study support the conclusions drawn previously.

Figs. 5 and 6 demonstrate the accuracy of the results by comparing the non-uniform model (LL and PL) and the uniform model (UL) of loading for normal and tangential stresses, confirming the linearity of the obtained gaits. Fig. 7 shows a linear relationship between the FGM model and the homogeneous model for displacements influenced by different loads, indicating the compatibility of the proposed models.

4. Conclusions

This study develops an exact two-dimensional plane elasticity solution for a functionally graded cantilever beam using the semi-inverse method. One of its principal strengths is the rigor of the formulation, which consistently incorporates the continuous variation of material properties through the beam thickness. Unlike classical beam theories, the proposed approach provides a more accurate and comprehensive description of both stress and displacement fields under a wide range of loading scenarios. In particular, it explicitly accounts for normal and shear tractions, concentrated forces, as well as end moments, thereby offering a unified and physically consistent framework. The inclusion of various load distributions uniform, linear, and parabolic—further enhances the versatility and applicability of the model.

The results highlight the pronounced influence of both loading conditions and material gradation on the mechanical response of the beam. It is shown that stiffer gradation profiles significantly improve structural stability and reduce deflections, whereas more compliant configurations lead to larger displacements. Furthermore, the analysis reveals that increasing positive gradation indices amplifies the peak normal stresses, while shear stress distributions remain significant and exhibit a symmetric pattern across the thickness. The formulation also successfully captures the effects of concentrated loads and end moments, which induce localized stress concentrations and influence the global deformation behavior.

An additional strength of the study lies in the smooth transition of the solution to the homogeneous limit, which confirms the robustness and consistency of the analytical model. Moreover, the generality of the proposed solution allows it to accommodate arbitrary material gradation profiles, making it a powerful reference for benchmarking numerical simulations and for supporting the development of simplified analytical approaches for functionally graded structures.

Future work may extend the present formulation to more complex scenarios, including thermo-elastic effects, dynamic loading conditions, and nonlinear material behavior. In addition, the approach could be adapted to different structural configurations, such as plates and shells, as well as to multi-dimensional gradation patterns. Such developments would further enhance the applicability of the model in advanced engineering design and optimization of graded materials.

References

1. Bousmaha, K., Belalia, S.A., Chorfi, S.M., Tounsi, A., Al-Osta, M.A., Alluqmani, A.E. (2026). On the dynamic behavior of plates made of porous advanced materials reinforced with carbon nanotubes using ap-version of finite element method. Mechanics Based Design of Structures and Machines, 54(1), 2534679. https://doi.org/10.1080/15397734.2025.2534679.
2. Daouadji, T.H., Adim, B., Alluqmani, A.E., Tayeb, B. (2026). Aluminum-wooden beam bonded by carbon fiber reinforced polymer: analysis and modeling. Coupled Systems Mechanics, 15(1), 1. https://doi.org/10.12989/csm.2026.15.1.001.
3. Rebaia, B., Tidjani, M., Lakhemissi, T., Meradjah, M., Tounsi, A., Alluqmani, A.E., ... Mahmoud, S.R. (2026). Investigation study of isotropic porous FG spherical shells using a refined higher-order shear deformation theory. Geomechanics and Engineering, 44(6), 775-795. https://doi.org/10.12989/gae.2026.44.6.775.
4. Daouadji, T.H. (2017). Analytical and numerical modeling of interfacial stresses in beams bonded with a thin plate. Advances in Computational Design, 2(1), 57-69. https://doi.org/10.12989/acd.2017.2.1.057.
5. Gawah, Q., Al-Osta, M.A., Shafique, M.T., Bourada, F., Tounsi, A. (2026). Stability analysis of graphene-reinforced functionally graded plates on elastic foundations under different in-plane loads. Results in Engineering, 109730. https://doi.org/10.1016/j.rineng.2026.109730.
6. Maya, H.D., Tahar, H.D., Tayeb, B. (2026). A new improved solution to reduce the shear stress interface of a steel beam strengthened with composite materials. Coupled Systems Mechanics, 15(1), 47. https://doi.org/10.12989/csm.2026.15.1.047.
7. Daouadji, T.H., Henni, A.H., Tounsi, A., El Abbes, A.B. (2013). Elasticity solution of a cantilever functionally graded beam. Applied Composite Materials, 20(1), 1-15. https://doi.org/10.1007/s10443-011-9243-6.
8. Mohamed, S.M., Youzera, H., Tounsi, A., Selim, M.M. (2025). Free vibrations analysis of a functionally graded honeycomb (FGH) Sandwich cylindrical shell using a quasi-3D theory. International Journal of Structural Stability and Dynamics, 2750159. https://doi.org/10.1142/S0219455427501598.

9. Daouadji, T.H., Benferhat, R., Abbes, B., Rabahi, A., Bensatallah, T., Abbes, F. (2025). Mechanical behavior of steel-concrete composite boxes reinforced with composite materials: Analysis and modeling. Structural Engineering and Mechanics, 95(5), 341-355. https://doi.org/10.12989/sem.2025.95.5.341.
10. Boulahbal, Y., Bouzid, T., Mamen, B., Bouhadra, A., Boutrid, A., Tounsi, A., Benrahou, K.H. (2025). On the bending behavior of nonhomogeneous nanoscale beams under nonlinear hygro-thermo-mechanical loading. Acta Mechanica, 236(5), 2921-2941. https://doi.org/10.1007/s00707-025-04293-x.
11. Maya, H.D., Tahar, H.D., Tayeb, B. (2026). A new improved solution to reduce the shear stress interface of a steel beam strengthened with composite materials. Coupled Systems Mechanics, 15(1), 47. https://doi.org/10.12989/csm.2026.15.1.047.
12. Mohammadimehr, M. (2024). The effect of a nonlocal stress-strain elasticity theory on the vibration analysis of Timoshenko sandwich beam theory. Advances in Nano Research, 17(3), 275-284. https://doi.org/10.12989/anr.2024.17.3.275.
13. Saidi, H., Tounsi, A., Bourada, F., Tounsi, A.A.B.A., Al-Juboori, F.I.S. (2024). Vibrational behavior of porous composite laminated plates using four unknown integral shear deformation theory. Steel and Composite Structures, 52(3), 249. https://doi.org/10.12989/scs.2024.52.3.249.
14. Laoud, B., Benyoucef, S., Bachiri, A., Bouiadjra, R.B., Tounsi, A., Selim, M.M., Saad, H.A. (2024). A comprehensive computational approach to assess the influence of the material composition on vibration, bending and buckling response of FG beam lying on viscoelastic foundation. Steel and Composite Structures, 52(1), 45-56. https://doi.org/10.12989/scs.2024.52.1.045.
15. Garg, A., Belarbi, M.O., Li, L., Chalak, H.D., Tounsi, A., Zenkour, A.M. (2024). Comparative study on the buckling analysis of exponential, power and sigmoidal sandwich FGM plates under hygro-thermal conditions. Advances in Materials Research, 13(6), 431-462. https://doi.org/10.12989/amr.2024.13.6.431.
16. Tang, C., Dui, G., Fu, Y. (2025). Elasticity solutions for functionally graded beams with arbitrary distributed loads. Composite Structures, 351, 118578. https://doi.org/10.1016/j.compstruct.2024.118578.
17. El-Shahrany, H.D., Zenkour, A.M. (2024). Control of dynamic response of the functionally graded smart sandwich beam coupled variable Kelvin–Voigt–Pasternak's model. Ain Shams Engineering Journal, 15(3), 102476. https://doi.org/10.1016/j.asej.2023.102476.
18. Mahmoud, S.R., Ghandourah, E.I., Algarni, A.H., Balubaid, M.A., Tounsi, A., Tounsi, A., Bourada, F. (2023). Stability investigation of symmetrically porous advanced composites plates via a novel hyperbolic RPT. Steel and Composite Structures, 46(4), 471. https://doi.org/10.12989/scs.2023.46.4.471.
19. Adim, B., Daouadji, T.H., Alluqmani, A.E. (2025). Study and analysis of the mechanical response of Carbon/Glass hybrid composite plates. Coupled Systems Mechanics, 14(6), 531. https://doi.org/10.12989/csm.2026.14.6.531.
20. Daouadji, T.H. (2013). Analytical analysis of the interfacial stress in damaged reinforced concrete beams strengthened by bonded composite plates. Strength of Materials, 45(5), 587-597. https://doi.org/10.1007/s11223-013-9496-4.
21. Wang, M., Liu, Y. (2010). Analytical solution for bi-material beam with graded intermediate layer. Composite Structures, 92(10), 2358-2368. https://doi.org/10.1016/j.compstruct.2010.03.013.
22. Choi, S.H., Lee, K.H., Kim, J.H., Lee, S.H., Kim, J., Kim, K.S. (2025). Behavior of pipe rack structures under blast loads. Computers and Concrete, 36(6), 613. https://doi.org/10.12989/cac.2025.36.6.613.
23. NS, N.P., Kaythry, P., Sangeetha, P. (2025). Deep learning based high strength concrete prediction model. Computers and Concrete, 36(6), 667. https://doi.org/10.12989/cac.2025.36.6.667.
24. Kebir, T., Kettaf, F.Z., Daikh, A.A., Benguediab, S., Hamdi, A., Ahmed, H.M., ... Eltaher, M.A. (2025). On the buckling response of FG-CNT fiber-reinforced composite laminated shells. Computers and Concrete, 36(5), 507-522. https://doi.org/10.12989/cac.2025.36.5.507.
25. Reddy, J.N., Ruocco, E., Loya, J.A., Neves, A.M. (2021). Theories and analysis of functionally graded beams. Applied Sciences, 11(15), 7159. https://doi.org/10.3390/app11157159.
26. Songsuwan, W., Wattanasakulpong, N., Vo, T.P. (2022). Nonlinear vibration of third-order shear deformable FG-GPLRC beams under time-dependent forces: Gram–Schmidt–Ritz method. Thin-Walled Structures, 176, 109343. https://doi.org/10.1016/j.tws.2022.109343.

27. Sun, S.L., Zhang, X.Y., Li, X.F. (2024). A consistent shear beam theory for free vibration of functionally graded beams based on physical neutral plane. Mechanics of Advanced Materials and Structures, 31(16), 3844-3854. https://doi.org/10.1080/15376494.2023.2185709.
28. Wang, M., Liu, Y. (2010). Analytical solution for bi-material beam with graded intermediate layer. Composite Structures, 92(10), 2358-2368. https://doi.org/10.1016/j.compstruct.2010.03.013.
29. Xu, Y., Yu, T., Zhou, D. (2014). Two-dimensional elasticity solution for bending of functionally graded beams with variable thickness. Meccanica, 49(10), 2479-2489. https://doi.org/10.1007/s11012-014-9958-1.
30. Yang, Q., Zheng, B., Zhang, K., Zhu, J. (2013). Analytical solution of a bilayer functionally graded cantilever beam with concentrated loads. Archive of Applied Mechanics, 83(3), 455-466. https://doi.org/10.1007/s00419-012-0693-6.
31. Zohra, A., Rabia, B., Tahar, H.D. (2024). Study and analysis of porosity distribution effects on the buckling behavior of functionally graded plates subjected to diverse thermal loading. Coupled Systems Mechanics, 13(2), 115-132. https://doi.org/10.12989/csm.2024.13.2.115.
32. Akbas, S.D. (2020). Dynamic analysis of a laminated composite beam under harmonic load. Coupled Systems Mechanics, 9(6), 563-573. https://doi.org/10.12989/csm.2020.9.6.563.
33. Aboudi, J., Arnold, S.M., Pindera, M.J. (1994). Response of functionally graded composites to thermal gradients. Composites Engineering, 4(1), 1-18. https://doi.org/10.1016/0961-9526(94)90003-5.
34. Yu, T., Zhong, Z. (2007). Bending analysis of a functionally graded piezoelectric cantilever beam. Science in China Series G: Physics, Mechanics and Astronomy, 50(1), 97-108. https://doi.org/10.1007/s11433-007-2006-6.
35. Malikan, M., Eremeyev, V.A. (2020). A new hyperbolic-polynomial higher-order elasticity theory for mechanics of thick FGM beams with imperfection in the material composition. Composite Structures, 249, 112486. https://doi.org/10.1016/j.compstruct.2020.112486.
36. Bourada, F., Amara, K., Bousahla, A.A., Tounsi, A., Mahmoud, S.R. (2018). A novel refined plate theory for stability analysis of hybrid and symmetric S-FGM plates. Structural Engineering and Mechanics, 68(6), 661-675. https://doi.org/10.12989/sem.2018.68.6.661.
37. Nebab, M., Atmane, H.A., Bennai, R. (2024). Investigating wave propagation in sigmoid-FGM imperfect plates with accurate Quasi-3D HSDTs. Steel and Composite Structures, 51(2), 185-202. https://doi.org/10.12989/scs.2024.51.2.185.
38. Henni, A.H., Daouadji, T.H. (2025). Effect of boundary conditions for functionally graded beams under uniformly distributed load. Coupled Systems Mechanics, 14(3), 231-245. https://doi.org/10.12989/csm.2025.14.3.231.
39. Adim, B., Daouadji, T.H., Mekid, R. (2025). Analysis of the mechanical behavior of functionally graded plates: Effect of boundary conditions and micromechanical models. Structural Engineering and Mechanics, 95(1), 31-42. https://doi.org/10.12989/sem.2025.95.1.031.
40. Daouadji, T.H., Abbès, F., Bensatallah, T., Abbès, B. (2025). Analytical and Numerical Investigation of Adhesive-Bonded T-Shaped Steel–Concrete Composite Beams for Enhanced Interfacial Performance in Civil Engineering Structures. Inventions, 10(4), 61. https://doi.org/10.3390/inventions10040061.
41. Sankar, B.V. (2001). An elasticity solution for functionally graded beams. Composites Science and Technology, 61(5), 689-696. https://doi.org/10.1016/S0266-3538(01)00007-0.
42. Zhu, H., Sankar, B.V. (2004). A combined Fourier series–Galerkin method for the analysis of functionally graded beams. Journal of Applied Mechanics, 71(3), 421-424. https://doi.org/10.1115/1.1751184.
43. Houari, M.S.A., Bessaim, A., Merzouki, T., Daikh, A., Garg, A., Tounsi, A., ... Belarbi, M.O. (2024). Shear correction factors of a new exponential functionally graded porous beams. Structural Engineering and Mechanics, 89(1), 1-11. https://doi.org/10.12989/sem.2024.89.1.001.
44. Daouadji, T.H., Abbès, B., Bensatallah, T., Abbès, F. (2025). Analysis of interface sliding in a composite I-steel–concrete beam reinforced by a composite material plate: the effect of concrete–steel connection modes. Journal of Composites Science, 9(6), 273. https://doi.org/10.3390/jcs9060273.
45. Eiadtrong, S., Nguyen, T.N., Wattanasakulpong, N. (2024). Nonlinear vibration of sandwich beams made of FGM faces and FGP core under multiple moving loads using a quasi-3D theory. Engineering Structures, 316, 118575. https://doi.org/10.1016/j.engstruct.2024.118575.

46. Kim, W.W., Moon, J.H. (2025). Simple model for predicting compressive strength of cement composites using carbon nanotubes based on cement hydration. Computers and Concrete, 36(5), 605. https://doi.org/10.12989/cac.2025.36.5.605.
47. Tahar, H.D., Henni, A.H. (2026). Elasticity-based analysis of bigraded FGM beams subjected to shear loading. Coupled Systems Mechanics, 15(2), 157. https://doi.org/10.12989/csm.2025.14.2.183.
48. Tahar, H.D., Abbes, B., Bensatallah, T., Abbes, F. (2026). Improved approach for composite steel-concrete slab continuous beams: Analysis of interfacial sliding stresses. Computers and Concrete, 37(4), 699-716. https://doi.org/10.12989/cac.2026.37.4.699.
49. Tayeb, B., Tahar, H.D., Boussad, A., Aberezak, R., Rabia, B., Fazilay, A. (2026). Analysis behavior of composite cellular steel-concrete beams reinforced by composite plate. Earthquakes and Structures, 30(2), 131. https://doi.org/10.12989/eas.2026.30.2.131.
50. Benguediab, S., Kettaf, F. Z., Sehoul, M., Bourada, F., Tounsi, A., Benguediab, M. (2023). Influences of hygrothermal environment and fiber orientation on shear correction factor in orthotropic composite beams. Coupled Systems Mechanics, 12(2), 151-165. https://doi.org/10.12989/csm.2023.12.2.151.
51. Hung, C.C., Nguyen, T. (2023). Aviation stability analysis with coupled system criterion of theoretical solutions. Coupled Systems Mechanics, 12(3), 221-239. https://doi.org/10.12989/csm.2023.12.3.221.
52. Ellali, M., Amara, K., Bouazza, M. (2024). Thermal buckling of porous FGM plate integrated surface-bonded piezoelectric. Coupled Systems Mechanics, 171-186. https://doi.org/10.12989/csm.2024.13.2.171.
53. Rizov, V.I. (2021). Delamination analysis of multilayered beams exhibiting creep under torsion. Coupled Systems Mechanics, 10(4), 317-331. https://doi.org/10.12989/csm.2021.10.4.317.
54. Huang, D.J., Ding, H.J., Chen, W.Q. (2007). Piezoelasticity solutions for functionally graded piezoelectric beams. Smart Materials and Structures, 16(3), 687-695. https://doi.org/10.1088/0964-1726/16/3/015.
55. Ma, H. (2020). Rational approach for higher-order shear deformation beam theories. Composite Structures, 251, 112599. https://doi.org/10.1016/j.compstruct.2020.112599.
56. Zahedinejad, P., Zhang, C., Zhang, H., Ju, S. (2020). A comprehensive review on vibration analysis of functionally graded beams. International Journal of Structural Stability and Dynamics, 20(04), 2030002. https://doi.org/10.1142/S0219455420300025.
57. Adim, B., Daouadji, T.H., Bekda, K. (2025). Micromechanical model-based analysis of porous functionally graded plates behavior using refined higher-order theory. Advances in aircraft and spacecraft science, 12(2), 95-115. https://doi.org/10.12989/aas.2025.12.2.095.
58. Tahar, H.D., Boussad, A., Abderezak, R., Rabia, B., Fazilay, A., Belkacem, A. (2019). Flexural behaviour of steel beams reinforced by carbon fibre reinforced polymer: Experimental and numerical study. Structural Engineering and Mechanics, 72(4), 409-420. https://doi.org/10.12989/sem.2019.72.4.409.
59. Henni, A.H., Daouadji, T.H. (2025). Analysis and modeling of the behavior of exponentially graded cantilever beams loaded by various parabolic distribution loads. Structural Engineering and Mechanics, 95(1), 43-50. https://doi.org/10.12989/sem.2025.95.1.043.
60. Zhong, Z., Yu, T. (2006). Two-dimensional analysis of functionally graded beams. AIAA Journal, 44(12), 3160-3160. https://doi.org/10.2514/1.26674.
61. Tang, C., Dui, G., Fu, Y. (2024). Explicit determination for exact solutions of elastic rectangular beams. International Journal of Mechanics and Materials in Design, 20(6), 1269-1289. https://doi.org/10.1007/s10999-024-09714-8.